Analytical Model to Study the Electrostatic Resonance of Sub-Wavelength Radially Inhomogeneous Negative Permittivity Spheres

Vincent Laquerbe*, Romain Pascaud*, Thierry Callegari†, Laurent Liard†, and Olivier Pascal†
* Institut Supérieur de l'Aéronautique et de l'Espace (ISAE-SUPAERO), Université de Toulouse, 31055 Toulouse
† LAPLACE, CNRS, UPS, INP, Université de Toulouse, 31400 Toulouse, France
Email: vincent.laquerbe@isae.fr

***Abstract*—This paper presents an analytical model to study the electrostatic scattering of sub-wavelength radially inhomogeneous spheres whose permittivity can be expressed as a general polynomial function of the radial distance r. This technique is particularly well suited to characterize the electrostatic resonance, also known as surface plasmon resonance, of radially inhomogeneous negative permittivity spheres.**

***Index Terms*—Sub-Wavelength Inhomogeneous Resonator, Negative Permittivity Spheres, Surface Plasmon Resonance.**

I. Introduction

SUB-WAVELENGTH particles are known to exhibit scattering peculiarities when their relative permittivity reach negative values [1]. Indeed, strong electrostatic resonance occurs in homogeneous sphere when $\varepsilon_r = -2$ [2], [3]. This specific feature has been suggested to design microwave electrically small antennas [4], optical nanoantennas [5], [6], or to study atmospheric re-entry blackout problem [7], [8]. Although many studies on this effect have been performed assuming a homogeneous sphere, it is noteworthy to derive radially inhomogeneous models.

The EM scattering of a radially inhomogeneous dielectric sphere has been widely studied through Mie theory [9]–[12], but these approaches usually require advanced numerical techniques with extensive computational analysis. When considering sub-wavelength spheres, it is usually more convenient to focus on the electrostatic scattering problem, thus simplifying the problem to the resolution of the Laplace equation. In this way, piecewise multilayered models have been proposed to analyze sub-wavelength radially inhomogeneous spheres [13]. However, they usually misrepresent the electrostatic resonance and its inherent local field amplifications [12]. To that extent, specific models have been developed for continuous media whose permittivity is a linear or single-powered function of the radial distance r [14], [15].

In this paper, an analytical model is proposed to study the electrostatic resonance of sub-wavelength radially inhomogeneous spheres whose permittivity is expressed as a general polynomial function of the radial distance r.

II. Theoretical Modeling

A. Statement of the problem

The general problem is depicted in Fig. 1. It consists in the EM scattering of a sub-wavelength radially inhomogeneous sphere of radius a immersed in a vertically polarized electric field $\vec{E_0}$. Its frequency-dependent relative permittivity is represented by the following lossless Drude model [16]:

$$\varepsilon_r(r,\omega) = 1 - \frac{\omega_p^2(r)}{\omega^2} \tag{1}$$

where ω is the angular frequency of the incident wave and ω_p is the plasma angular frequency that accounts for the radial inhomogeneity of the sphere. It is assumed that $\omega_p(r)$ can be expressed as a polynomial function of the radial distance r. Thus, the relative permittivity of the sphere is also defined as a polynomial function of r whose general expression at a given angular frequency ω_0 is:

$$\varepsilon_r(r,\omega_0) = \varepsilon_{r,0} + \varepsilon_{r,1} r + \varepsilon_{r,2} r^2 + \cdots + \varepsilon_{r,m} r^m \tag{2}$$

where all $\varepsilon_{r,i}$ are real coefficients.

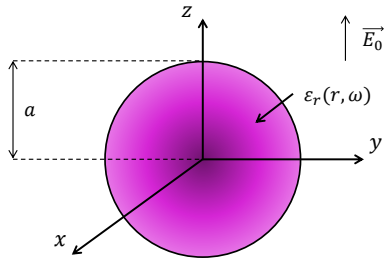

Fig. 1. EM scattering of a radially inhomogeneous sphere immersed in a vertically polarized electric field $\vec{E_0}$

As long as the radius a of the sphere is small compared with the free-space wavelength of the incident wave, i.e., $ka \ll 1$ where k is the free-space wavenumber, the problem can be reduced to the computation of the scalar potential $\Phi(r,\theta,\phi)$ using the Laplace equation. Note that the influence of a on the electrostatic assumption has been raised in [17].

The method of separation of variables allows us to quickly find the angular component of Φ. Only the first spherical harmonic is non-zero, which highlights a dipole-like response of the sphere [13]. Finally, the scalar potential in each region is thus expressed as

$$\Phi_{sphere}(r,\theta) = R_1(r)\cos\theta \tag{3a}$$

$$\Phi_{out}(r,\theta) = -E_0 r\cos\theta + \frac{B_{out}}{r^2}\cos\theta \tag{3b}$$

where B_{out}, the dipole coefficient in the outer region, and $R_1(r)$ are to be determined.

B. Solution for the scalar potential

Inside the sphere, the Laplace equation for the radial component $R_1(r)$ does not reduce to a single power of r, as it is the case for a homogeneous sphere [15], and the following general equation must be solved:

$$\underbrace{\varepsilon_r(r)\frac{d}{dr}\left(r^2\frac{dR_1}{dr}\right)}_{T_1}+\underbrace{r^2\frac{d\varepsilon_r(r)}{dr}\frac{dR_1}{dr}}_{T_2}-\underbrace{2\varepsilon_r(r)R_1}_{T_3}=0 \tag{4}$$

Assuming a general normalized power-law solution $R_1(r)=\sum_l C_l r^l$, only positive powers of r are non-zero as negative values exhibit a pole at the origin. For the sake of simplicity, (4) can be normalized to the first term in the expansion of ε_r so that, with no loss of generality, we can assume that

$$\tilde{\varepsilon}_r(\tilde{r})=\sum_{q=0}^{m} b_q\tilde{r}^q \quad \text{where} \quad \tilde{r}=\frac{r}{a} \quad \text{and} \quad b_q=\frac{\varepsilon_{r,q}}{\varepsilon_{r,0}}a^q. \tag{5}$$

Similarly, R_1 is normalized to the first term C_0 in its expansion so that (4) is now solved with:

$$\tilde{R}_1(\tilde{r})=\sum_{l\geqslant 0}\tilde{C}_l\tilde{r}^{l+s}, \quad \text{with} \quad \tilde{C}_l=\frac{C_l}{C_0}a^{l+s} \tag{6}$$

where s is a positive integer that is found by polynomial identification on the lowest power of $\tilde{r}$ (which is $\tilde{r}^s$) in the development of (4). This leads to the following characteristic equation, as presented in [15]:

$$\Big[s(s+1)-2\Big]=0 \tag{7}$$

From (7), it is clear that $s=1$. Developing (4) according to the powers of $\tilde{r}$ and substituting each power to obtain only sums of $\tilde{r}^{l+1}$, the $T_{1,2,3}$ terms can be expressed as follows:

$$\begin{aligned}
T_1&=\sum_{l\geqslant 0}\left(\sum_{q=0}^{m}(l+1-q)(l+2-q)b_q\tilde{C}_{l-q}\right)\tilde{r}^{l+1}\\
T_2&=\sum_{l\geqslant 0}\left(\sum_{q=1}^{m}q(l+1-q)b_q\tilde{C}_{l-q}\right)\tilde{r}^{l+1}\\
T_3&=\sum_{l\geqslant 0}\left(\sum_{q=0}^{m}2b_q\tilde{C}_{l-q}\right)\tilde{r}^{l+1}
\end{aligned} \tag{8}$$

By identification and after brief manipulations, the following recurrence relation can be derived:

$$\tilde{C}_l+\sum_{q=1}^{\min(l,m)}\frac{l^2+3l-lq-2q}{l(l+3)}b_q\tilde{C}_{l-q}=0 \tag{9}$$

Dong *et al.* first suggested this approach in [15] but restrained the resolution to linear and single-powered radial profile. Though, when considering linear profile, i.e., $m=1$, (9) becomes:

$$\tilde{C}_l+\frac{l^2+2l-2}{l(l+3)}b_1\tilde{C}_{l-1}=0 \tag{10}$$

which is consistent with [15]. In the end, using (3) and the boundary conditions at $r=a$ on the scalar potential and the electric displacement field between the sphere and the surrounding medium restore E_0 and yield to:

$$C_0=\frac{-3E_0}{\varepsilon_r(a)\left.\frac{d\tilde{R}_1}{d\tilde{r}}\right|_{\tilde{r}=1}+2\tilde{R}_1(1)} \tag{11}$$

and:

$$B_{out}=\frac{\varepsilon_r(a)\left.\frac{d\tilde{R}_1}{d\tilde{r}}\right|_{\tilde{r}=1}-\tilde{R}_1(1)}{\varepsilon_r(a)\left.\frac{d\tilde{R}_1}{d\tilde{r}}\right|_{\tilde{r}=1}+2\tilde{R}_1(1)}a^3E_0 \tag{12}$$

When all $b_{q>0}$ are zeros, i.e., for a homogeneous sphere, it can be seen from the recurrence relation (9) that all $\tilde{C}_{l>0}$ are also zeros and $\tilde{R}_1(\tilde{r})=\tilde{r}$. This way, B_{out} simplifies to:

$$B_{out}=\frac{\varepsilon_{r,0}-1}{\varepsilon_{r,0}+2}a^3E_0 \tag{13}$$

which is the classic dipole factor of a homogeneous sphere that highlights the electrostatic resonance for $\varepsilon_{r,0}=-2$ [1].

This model can be further extended to study more sophisticated structures involving any radially inhomogeneous sphere embedded inside multiple dielectric layers. In this case, the scalar potential is likely derived applying the same boundary conditions as before at the interfaces between each different medium [13].

C. Discussion on the validity of the proposed model

The main benefit of considering a generic polynomial permittivity profile inside the sphere, as in (2), lies in its ability to uniformly approximate any continuous function on a closed interval according to the Stone-Weierstrass theorem.

However, as it complicates the resolution of the Laplace equation, the series $\tilde{R}_1$ may not have a finite limit. It is therefore necessary to find a domain of convergence $\mathcal{D}$ within which $\tilde{R}_1$ is unambiguous and well-defined. It is here proven that a valid domain of convergence is:

$$\mathcal{D}=\left\{\{b_i\}_{i\in[0,m]}\ |\quad f_b=\sum_{q=1}^{m}|b_q|<1\right\} \tag{14}$$

Developing (9) for the first $m-1$ terms, it can be seen step-by-step that each term is smaller than f_b in absolute value, and thus by recurrence:

$$\forall l\geqslant 1, \quad \left|\tilde{C}_l\right|\leqslant\sum_{q=1}^{m}|b_q| \tag{15}$$

Likewise, considering the following terms ($l>m$) from (9) and using the inequality derived above by recurrence, a new upper bound can be derived:

$$\left|\tilde{C}_{l>m}\right|\leqslant\sum_{q=1}^{m}|b_q|\left|\tilde{C}_{l-q}\right| \quad \leqslant\sum_{q=1}^{m}|b_q| \tag{16}$$

The same technique can be used for each sequence of m terms. Between each sequence the upper bound is tightened by f_b so that:

$$\forall l > 0, \quad \left|\tilde{C}_l\right| \leqslant \left(\sum_{q=1}^{m} |b_q|\right)^{\lfloor l/m \rfloor + 1} \tag{17}$$

where $\lfloor \cdot \rfloor$ denotes the floor function. Eq. (17) proves that $\{\tilde{C}_l\}_{l>0}$ are converging to 0. Now grouping each sequence of m terms in the expression of $\tilde{R}_1$ and using (17), an upper bound can be derived:

$$\begin{aligned}
\left|\tilde{R}_1\right| &\leqslant \sum_{l=0}^{m-1} \left|\tilde{C}_l\right| + \sum_{l=m}^{2m-1} \left|\tilde{C}_l\right| + \sum_{l=2m}^{3m-1} \left|\tilde{C}_l\right| \cdots \\
\left|\tilde{R}_1\right| &\leqslant m + m\left(\sum_{q=1}^{m} |b_q|\right) + m\left(\sum_{q=1}^{m} |b_q|\right)^2 \cdots \\
\left|\tilde{R}_1\right| &\leqslant m\frac{1}{1-f_b}
\end{aligned}$$

In the end, $\tilde{R}_1$ is bounded and its terms are converging to 0. Thus, as it takes its values in a Cauchy space, namely the closed interval $[0, 1]$, it converges.

As it will be raised in Section III-A, the theoretical case of a material whose permittivity is locally equal to 0 is singular. Mathematically, if at a certain radial distance $\tilde{r}_1$ in the sphere $\tilde{\varepsilon}_r(\tilde{r}_1) = 0$, then (5) can be written as:

$$\tilde{\varepsilon}_r(\tilde{r}_1) = 1 + \sum_{q=1}^{m} b_q \tilde{r}_1^q = 0 \tag{18}$$

which yields:

$$1 = \left|\sum_{q=1}^{m} b_q \tilde{r}_1^q\right| \leqslant \sum_{q=1}^{m} |b_q| = f_b \tag{19}$$

In other words, if the permittivity is locally equal to 0 inside the sphere, the domain of convergence $\mathcal{D}$ is no longer respected and the proposed model is not applicable.

III. Numerical Results

A. Computation of the resonant frequency

The following non-trivial profile for ω_p is now considered as an example, with $a = 10$ mm:

$$\frac{\omega_p^2(r)}{\omega_p^2(0)} = 1 - \frac{1}{20}\left(\frac{r}{a}\right) - \frac{1}{10}\left(\frac{r}{a}\right)^2 - d\left(\frac{r}{a}\right)^3 \tag{20}$$

where $\omega_p(0)$ is the plasma angular frequency at the center. The coefficient d is a smaller-than-1 positive integer that will vary to study the reliability of the model and prove its necessity.

Solving the Laplace equation with the proposed algorithm, the normalized dipole coefficient $|B_{OUT}|$ from (3) is calculated and represented in Fig. 2 as a function of the electrical size ka of the sphere and $\omega_p(0)$ for $d = 0.5$. The dipole coefficient strongly increases locally which reflects a dipole resonance. For example, using Fig. 2 for $\omega_p(0) = 10^{10}$ rad.s^{-1}, the resonance occurs at $ka = 0.155$, i.e. $f = 740$ MHz.

Note that the white area from Fig. 2 corresponds to divergent cases for which the permittivity is locally equal to 0, as seen in Section II-C. Anyhow, as the electrostatic resonance is obtained for purely negative permittivity sphere, the proposed algorithm allows either the computation of its resonant frequency assuming the material function ω_p or the opposite way.

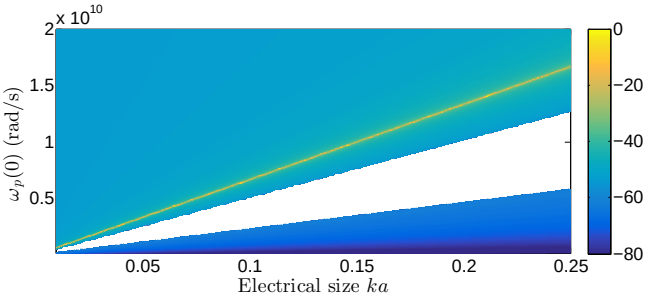

Fig. 2. Normalized dipole coefficient $|B_{OUT}|$ (in dB) calculated for different ka and $\omega_p(0)$ assuming the profile from (20) with $d = 0.5$. The dipole resonance is depicted by the yellow line.

B. Influence of the gradient on the resonance

As seen before, when $\omega_p(0)$ varies, the corresponding resonant electrical size ka changes similarly. Likewise, for a given $\omega_p(0)$, considering a different plasma angular frequency gradient shifts the resonant ka. Fig. 3 depicts this matter where the resonant parameters $\omega_p(0)$ and ka have been calculated for several profiles with different values of d, the normalized coefficient of the highest power of r in (20). These resonant sets of parameters have been compared with the classic homogeneous sphere that resonates when $\varepsilon_r = -2$. It is clear from Fig. 3 that the larger the gradient is (i.e., larger d), the stronger the shift from the homogeneous case is. This trend confirms the need to derive continuous models that deal with radial inhomogeneity, especially for resonant structures.

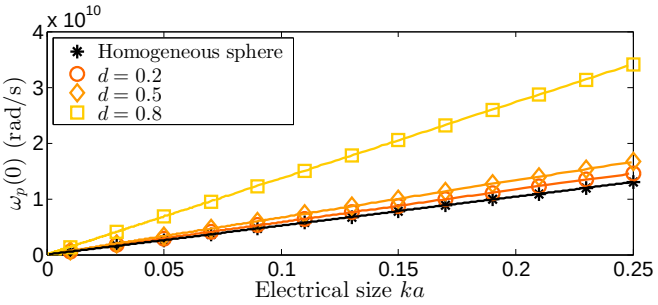

Fig. 3. Locus of $\{ka, \omega_p(0)\}$ exhibiting the dipole resonance, derived for the profile (20) with different d and for the homogeneous case $\omega_p(r) = \omega_p(0)$.

C. Comparison with full-wave simulation

Finally, the previously derived model is compared to numerical simulations held with the commercial full-wave software Ansys HFSS. The structure from Fig. 1 is considered with $ka = 0.05$ and $a = 10$ mm, as assumed in III-A. This defines the theoretical resonant frequency $f_{th} = 239$ MHz. The corresponding $\omega_p(0)$ that is required to obtain a resonant sphere is then computed from Fig. 3 for each d in (20).

Since inhomogeneous materials cannot be simulated with Ansys HFSS, the sphere must be split into several homogeneous parts. Considering radial inhomogeneity only, the sphere is modeled as N concentric spherical layers of uniform thickness a/N. These spherical layers are excited by a plane wave propagating along $\vec{y}$-direction, as depicted in Fig. 4.

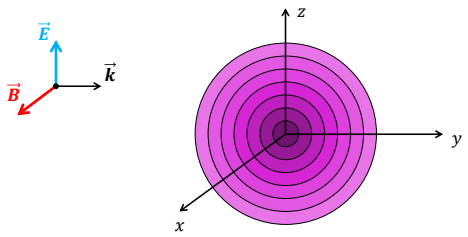

Fig. 4. Simulated sphere of N layers with constant permittivity in Ansys HFSS excited by a plane wave propagating along $\vec{y}$-direction. Note that 3 planes of symmetry were used and the sphere comprises at least 20000 tetrahedra (depending on the value of N).

The dielectric permittivity is supposed to be constant inside each spherical layer. To avoid numerical instabilities, small losses have been added which, assuming a lossy Drude model, leads to the following dispersive relative permittivity and bulk conductivity for each spherical layer in Ansys HFSS:

$$\varepsilon_{rn}(\omega) = 1 - \frac{\omega_{pn}^2}{\omega^2 + \nu^2}, \text{ and } \sigma_n(\omega) = \varepsilon_0 \frac{\omega_{pn}^2 \nu}{\omega^2 + \nu^2} \quad (21)$$

where $\nu = 0.01\omega_p(0)$ represents the losses and ω_{pn} the plasma angular frequency inside the n-th spherical layer and is equal to the median value of ω_p in this layer, computed with (20).

As the electrostatic resonance of a sphere results in a strong amplification of the electric field $\vec{E}$ at the poles, the numerical resonant frequency f_{num} is defined as the frequency which maximizes $|\vec{E}|$ at $z = a$. These calculations were performed for several values of N and compared to the analytical frequency f_{an} derived with the proposed model.

Fig. 5 represents the relative error $\Delta_f = |1 - f_{num}/f_{th}|$ in the estimation of f_{num} obtained for different N and d. Small N strongly misrepresent the electrostatic resonance of the radially inhomogeneous sphere because of numerical singularities that skew the computed electric field. Although increasing N prevents these numerical instabilities and provides decent results for small d, it is clear that piecewise multilayered representations are not suitable for large gradients.

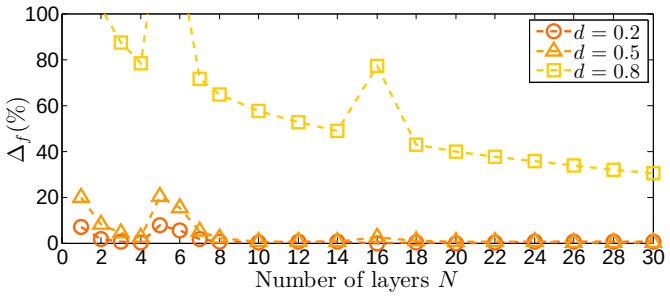

Fig. 5. Relative error (in %) in the evaluation of the resonant frequency using Ansys HFSS for different numbers of spherical layers N.

In our case, when d gets closer to 1, the sphere is strongly inhomogeneous and the numerical convergence is extremely slow. The proposed model overcomes this issue and allows to easily compute the resonant frequency of any sub-wavelength radially inhomogeneous sphere.

IV. Conclusion

A generalized approach using polynomial graded relative permittivity profiles has been proposed to solve the Laplace equation inside sub-wavelength radially inhomogeneous negative permittivity spheres. This model provides an accurate estimation of the resonant frequency of such spheres. It has been compared with commercial numerical solver and appears to be well-suited to study their electrostatic resonance. An analytical criterion has also been established to ensure its reliability and convergence.

Acknowlegments

The authors would like to thank the French Defense Agency (DGA) for its financial support.

References

[1] C. F. Bohren and D. R. Huffman, *Absorption and Scattering of Light by Small Particles*. John Wiley & Sons, 1998.

[2] A. Alù and N. Engheta, "Polarizabilities and effective parameters for collections of spherical nanoparticles formed by pairs of concentric double-negative, single-negative, and/or double-positive metamaterial layers," *J. Appl. Phys.*, vol. 97, p. 094310, 2005.

[3] A. Sihvola, "Character of surface plasmons in layered spherical structures," *Prog. Electromagn. Res.*, vol. 62, pp. 317–331, 2006.

[4] H. R. Stuart and A. Pidwerbetsky, "Electrically small antenna elements using negative permittivity resonators," *IEEE Trans. Antennas Propag.*, vol. 54, no. 6, pp. 1644–1653, Jun. 2006.

[5] S. Kühn, U. Håkanson, L. Rogobete, and V. Sandoghdar, "Enhancement of single-molecule fluorescence using a gold nanoparticle as an optical nanoantenna," *Phys. Rev. Lett.*, vol. 97, p. 017402, Jul. 2006.

[6] M. Agio and A. Alù, *Optical Antennas*. Cambridge University Press, 2013.

[7] C. C. Lin and K. M. Chen, "Radiation from a spherical antenna covered by a layer of lossy hot plasma. Theory and experiment," *Proc. IEE*, vol. 118, no. 1, pp. 36–42, Jan. 1971.

[8] X. Gao and B. Jiang, "A matching approach to communicate through the plasma sheath surrounding a hypersonic vehicle," *J. Appl. Phys.*, vol. 117, no. 23, p. 233301, 2015.

[9] P. J. Wyatt, "Scattering of electromagnetic plane waves from inhomogeneous spherically symmetric objects," *Phys. Rev.*, vol. 127, pp. 1837–1843, Sep. 1962.

[10] E. Bilgin and A. Yapar, "Electromagnetic scattering by radially inhomogeneous dielectric spheres," *IEEE Trans. Antennas Propag.*, vol. 63, no. 6, pp. 2677–2685, Jun. 2015.

[11] R. A. Shore, "Scattering of an electromagnetic linearly polarized plane wave by a multilayered sphere," *IEEE Antennas Propag. Mag.*, vol. 57, no. 6, pp. 69–116, Dec. 2015.

[12] A. Shalashov and E. Gospodchikov, "Simple approach to electromagnetic scattering by small radially inhomogeneous spheres," *IEEE Trans. Antennas Propag.*, vol. 64, no. 9, pp. 3960–3971, Sep. 2016.

[13] A. Sihvola and I. V. Lindell, "Transmission line analogy for calculating the effective permittivity of mixtures with spherical multilayer scatterers," *J. Electromagn. Waves Applicat.*, vol. 2, no. 8, pp. 741–756, 1988.

[14] E.-B. Wei, Z.-D. Yang, and J.-B. Song, "Effective dielectric response of graded spherical composites," *Phys. Lett. A*, vol. 316, no. 6, pp. 419–423, Oct. 2003.

[15] L. Dong, G. Q. Gu, and K. W. Yu, "First-principles approach to dielectric response of graded spherical particles," *Phys. Rev. B*, vol. 67, p. 224205, 2003.

[16] M. A. Lieberman and A. J. Lichtenberg, *Principles of Plasma Discharges and Materials Processing*. John Wiley and Sons, 2005.

[17] Z. Mei and T. Sarkar, "A study of negative permittivity and permeability for small sphere," *IEEE Antennas Wireless Propag. Lett.*, vol. 12, pp. 1228–1231, 2013.